2017 IEEE International Conference on Systems, Man, and Cybernetics (SMC)
Banff Center, Banff, Canada, October 5-8, 2017

The Use of Thermal IR Array Sensor for Indoor Fall Detection

Akira Hayashida, Vasily Moshnyaga
Graduate School of Engineering,
Fukuoka University
8-19-1 Nanakuma, Jonan-ku
Fukuoka 8140180, Japan

Koji Hashimoto
Dept. Electronics Eng. & Computer Science
Fukuoka University
8-19-1 Nanakuma, Jonan-ku
Fukuoka 8140180, Japan

***Abstract*—This paper presents new approach for unobtrusive indoor fall detection by an IR thermal array sensor. Unlike existing methods that run fall detection at server and require high communication and processing rates, we perform fall detection within the sensor node by a computationally inexpensive algorithm that signals the server only when a fall occurs. Experiments with prototype design show that such formulation provides robust and real-time fall detection even in a noisy environment.**

Keywords—assistive technology; fall detection; IR array sensor; passive system

I. INTRODUCTION

A. Motivation

According to the World Health Organization [1] almost 1/3 of people aged 65+ and up to 42% of those aged 70+ experience fall accidents annually. Due to increasing fragility of human bodies with age, a fall may cause an elder a severe injury (hip fracture, head traumas, etc.) with a serious complication. The problem worsens for elders who live alone, as they might not be able to get up after a fall due to either an injury or declining muscular activity [2]. Hence, technologies capable of automatically detecting falls and sending an emergency call for a help are a social necessity.

Over the years various automatic fault detectors have been developed [3]-[5]. Wearable detectors (e.g. pendants or wrist-type devices) are inexpensive but must be worn all time which is a problem for users. Some question the need for device; others consider it an unwelcome admission of vulnerability [6]. Passive technologies use multiple sensors embedded into environment. They detect a human fall unobtrusively but rely on the sensor' range, ambient noise, are expensive and may increase privacy concerns (e.g. image based).

The main goal of this paper is to present an approach that contributes to passive fall detection technology based on infrared (IR) array sensors. An IR sensor (or thermopile) detects IR radiation from objects and converts its thermal energy to an electric voltage, proportional to the quantity of detected radiation. Due to ability to differentiate changes in IR flux, an array of thermopiles properly arranged on a chip, can detect moving objects, direction of movement, position and presence of motionless objects. It does not affect user' privacy, is small, reliable and inexpensive.

B. Related research

Small IR array sensors have already found use in many applications, such as biomedical devices, security, automotive and home appliances [8,9], object recognition [10], occupancy detection [11] and motion tracking [12]. Several studies have considered IR array sensors for human activity and fall detection. Kallur[13] combined IR array sensors with motion sensors for detecting human activities, such as walking, standing, sitting and sleeping. Sixsmith, et al. [14] studied wall mounted IR array sensors to detect falls of elderly people. Mashiyama, et al. advocated ceiling-placed IR array sensor for activity recognition [15] and fall detection [16]. Despite differences in implementation, all these solutions have several features in common. Namely, they use intense processing and data transfer, consume large power and can thus require wired power supply. Because power lines must be on walls [14] or ceiling [15-16], installing them without infringing the user comfort becomes expensive. Besides, the provided solutions assume an unchangeable environment and may eventually fail when electric appliances inside the monitored room are switched on.

C. Contribution

This work has two main contributions. The first one is a novel fall detection approach optimized to operate at varying backgrounds and with minimum computations and data transfers. The second contribution is a wireless fall-detection system that performs in real-time and has robust fall-detection accuracy regardless of noise imposed by room appliances.

The rest of the paper is organized as follows. The next section describes the proposed fall detection approach. Section III presents implementation and evaluation results. Section IV summarizes this work by conclusion.

II. THE PROPOSED FALL-DETECTION APPROACH

A. An Overview

The proposed approach is dedicated to automatically and unobtrusively track a person within a room environment and alert the caregiver if the fall incident occurs. We assume that the fall detection system has sensor nodes, mounted on ceiling, and wirelessly connected to a PC server through Xbee protocol, as shown in Fig.1. Each sensor node contains an 8x8 IR array

978-1-5386-1645-1/17/$31.00 ©2017 IEEE

Authorized licensed use limited to: University of Adelaide. Downloaded on September 03,2021 at 01:20:20 UTC from IEEE Xplore. Restrictions apply.

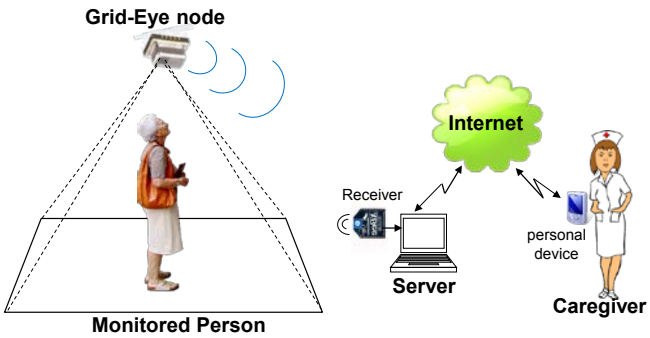

Figure 1. Illustration of the proposed fall detection system

sensor from Panasonic (marketed as Grid-EYE) [17] that captures the thermal radiation absorbed from the area below (60º viewing angle) and analyzes its content to detect whether it corresponds a human fall. If a human fall is detected, the node signals the server (receiver). The server records the event in local database, generates an alert message and sends it to the caregiver via the internet.

Our main target was a system that robustly detects human falls in real time and is easy to install and maintain. Wireless communications satisfy the installation requirements but elevate the node energy consumption to be a prime design concern. The energy consumed by the node is the sum of data processing energy, data transmission energy and idling energy. Because an XBee device requires 50mA@3.3V for a data transfer [18], i.e. more than a microcontroller, such as Arduino takes in normal (1.4mA) and sleep (50uA) modes @3.3V [19], [20] we minimize wireless transfers as much as possible. Namely, we perform fall detection inside the node, activating the wireless transmitter to signal the server only when a fall occurs. In addition, we reduce the number of fall detection operations, adopt a low processing rate (5fps) to save energy whenever possible.

The fall detection is done in four main steps shown in Fig.2. Below we discuss the steps in detail.

B. *The T-map acquisition*

The goal of this step is to capture the current IR thermal signature of the monitored area. The Grid-Eye array sensor measures thermal radiation from the scene and maps the temperature data to an 8x8 thermal image. We refer to a thermal image obtained at time t as T-map, $\mathbf{F}_t$, of the scene. Fig.3 illustrates T-maps obtained from a scene without a person (Fig3, a) and with a person standing (Fig.3, b). The squares here show the T-map pixels, numbers reveal temperatures (in Celsius) and color reflects the thermal amplitude.

In comparison to a conventional image, a T-map has several peculiarities. First, it is a low-resolution representation of a scene. For example, if the array sensor is 2.7m above the floor, a pixel of the T-map reflects the average temperature of area 35x35cm2 in size. Second, the T-map representation accuracy depends on the distance between the sensor and the subject. The closer the subject to the sensor, the more accurate

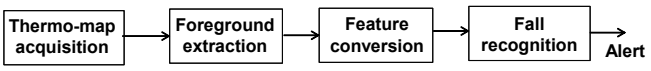

Figure 2. Functional diagram of the fall-detection process

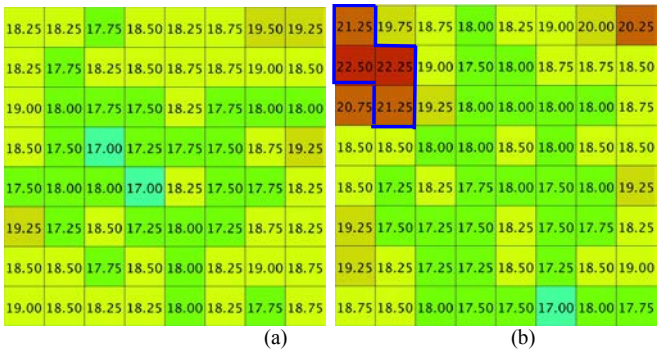

Figure 3. A T-map of a scene with no moving object (a) and a scene having a moving object (b)

are the temperature readings. However, as the distance from the sensor increases, the field of view of the sensor also increases. If the subject is far from the sensor, its angular size appears smaller to the sensor as the field of view is expanding; so the subject appears much smaller in the sensor detection zone. Third, as distance from the sensor grows, the heat signature produced by the sensor decreases due to the fact that the subject only partially covers the relevant pixels and the heat from the subject is blending with the background. This is further compounded by the fact that the IR radiation produced by a warm body decays as the distance to the sensor increases. These relationships make the effect of temperature lower than it should be, increasing the difficulty of identifying human poses at long distances. Finally, the T-map is very sensible to noise induced by objects in the room (e.g. computer, heater, etc.) as well as outside temperature. The noise is non-static and varies in time as the temperature of the objects is changing. Hence noise reduction is paramount to correct fall detection based on IR array-sensors.

C. *Foreground extraction*

This is a key step in providing proper information for accurate human fall detection in varying and noisy conditions. Our target here is to separate a human subject (which can be moving or stationary) from the passive objects in background. In order to differentiate a subject from passive warm objects such as computer, TV, heater, desk lamp, etc. we adopt the threshold based background separation method [21]. Amid other formulations, this method is less computationally expensive yet quite accurate.

We assume that background T-map, **B**, is determined at the system activation and then periodically updated as follows. If no motion has been observed in the sensor's field of view during a given time interval (λ), the current T-map, $\mathbf{F}_t$, becomes B. Otherwise, we take four pixels with the lowest temperatures in $\mathbf{F}_t$, compute variations of their temperatures relatively to B and then scale the pixels of B by adding $(-1)^S \times \alpha$ to their values. Here α is the average of the four variations; S=1

Authorized licensed use limited to: University of Adelaide. Downloaded on September 03,2021 at 01:20:20 UTC from IEEE Xplore. Restrictions apply.

if α is positive and S=0 otherwise. The modified B is stored in local memory.

The foreground extraction is done by subtracting the background, B, from the current temperature map, $\mathbf{F}_t$ and comparing the difference to a given threshold, θ_1.

A pixel (i,j) belongs to foreground if

$$D(i,j) = \left| \mathbf{F}_t(i,j) - \mathbf{B}(i,j) \right| \geq \theta_1, \qquad (1)$$

Else, it belongs to background. For example, if the T-maps in Fig.2 show **B** and $\mathbf{F}_t$, respectively, and $\theta_1=3$ than the foreground region $\mathbf{R} \epsilon \mathbf{F}_t$ covers four pixels in the left corner depicted by the bold line.

In the system, we set λ=15min (the typical threshold in appliance control [22]). If none of the pixels satisfy (1), the system returns to the initial step and waits for acquisition of next T-map. Otherwise it proceeds to the feature conversion and fall detection. The result of foreground extraction is represented by the upper-left (X_L,Y_U), the upper-right (X_R,Y_U), the lower-left (X_L,Y_W) and the lower-right (X_R, Y_W) points of the foreground region (R) and the maximal thermal difference (M) between corresponding regions in foreground and background.

D. Feature Conversion

This step converts the foreground temporal dynamic into a set features for fall detection. Unlike other human activities, a human fall is an abrupt action of fast motion velocity. To represent this peculiar action, we chose those features which provide good classification quality without large computational and memory overhead. The selected features are: the maximal temperature difference (M); the maximal motion distance (L), the duration of motion (Δ), and variance (ξ) of the maximal thermal difference between foreground and background over the time Δ.

1) The maximal thermal difference between the background and foreground pixels (M);

The closer the human subject to the sensor, the higher the difference D(i,j) in (1). For same person in standing and lying positions, the value of $M=Maximum\{D(i,j),\ i=0,..,7;\ j=0,..,7\}$ differs by several degrees and hence can classify a person lying on the floor. We compute *M* during the foreground extraction by iteratively selecting the maximum of those differences which satisfy (1). The procedure requires |**R**| extra comparisons, where |**R**| is the number of pixel in the foreground region **R**. For example, the maximum thermal difference in foreground region shown in Fig.3 (b) is *M*= 4.5.

2) Variance (ξ) of the maximal thermal difference.

A large variance (ξ) of the maximal thermal difference occurs when a person abruptly changes his/her position relatively to the sensor. Because old people usually move slowly, an abrupt change in maximal temperature reflects a fall. If $M(\mathbf{F}_t)$ and $M(\mathbf{F}_{t-1})$ are the maximum thermal differences computed for current and previous T-maps, respectively, then $\xi = \left| M(\mathbf{F}_t) - M(\mathbf{F}_{t-1}) \right|$.

3) The duration of activity (Δ) .

Unlike other human activities, a fall is characterized by fast motion velocity followed by no-motion. Our system captures T-maps every 0.2 sec. If FI and FN correspond to initial T-maps of two sequential actions, respectively, the duration of the first action (in seconds) is $\Delta = \left| N - I \right| \times 0.2$. Because a human fall is quick, an action tends to be a fall if its duration $\Delta \leq 1$ sec.

4) The motion distance (L)

For the given time window, Δ, the motion velocity represents the distance between same points of foreground at the start (I) and the end (N) of the window, i.e. $L = \left| \mathbf{R} \epsilon \mathbf{F}_I - \mathbf{R} \epsilon \mathbf{F}_N \right|$. We use a single point associated with the center of the foreground's bounding box. If (X_L,X_R) are the left- and the right-most columns of the foreground's bounding box, respectively, and (Y_U,Y_W) are the upper-most and the lower-most rows of the bounding box, respectively, the center point has coordinates (Xc,Yc), where $X_C=(X_R-X_L)/2$, and $Y_C=(Y_W-Y_U)/2$. Thus,

$$L = \sqrt{\left([X_C(t) - X_C(t+\Delta)]^2 + [Y_C(t) - Y_C(t+\Delta)]^2 \right)}, \qquad (2)$$

Because Δ is small, an action with a large value of L might be a fall.

Fig.4 illustrates snapshots of a human fall taken with a time interval of 0.2 sec. and the corresponding variation in foreground and the motion distance. For simplicity, the T-maps (below the photos) are given in a binary form, in which the foreground pixels (shown in red) are represented by 1 and the background pixels (shown in black) by 0. The motion distance (*L*) is depicted in yellow. The bold arrows show the motion in regards to the previous T-Map; the dotted arrow shows the total motion in the time Δ. As one can see, the motion distance (*L*) of a falling person is large indeed.

E. Fall Detection

The problem is formulated as follows: Given a feature vector {*M, ξ, Δ, L*}, which characterizes the temporal dynamics of the foreground region, determine whether it reflects a fall or a no-fall according to the trained classifiers $\Omega_1, \Omega_2, \ldots, \Omega_P$. The proposed solution algorithm (Fig.5) takes the foreground region ($\mathbf{R}_t$) and the maximum thermal difference (*M*) between the foreground and background pixels and computes coordinates (X_C,Y_C) of the central point of the region's bounding box. If $M<\theta_3$, the system assumes no person on the scene and returns to the T-map acquisition step. If $\theta_3<M<\theta_2$, it computes the duration of current activity (Δ), the motion distance (L) and the variance of the maximal thermal difference (*ξ*) based on the current time (N) and the maximal foreground temperature, M0, of the previous T-map (M0 is 0, initially). If they satisfy the given classifiers ($L<\theta_4$, $\Delta<\theta_5$, $\xi>\theta_6$) the current activity is assumed to be a fall. Otherwise, the system records the current time and coordinates (X_C, Y_C) of the central point of the foreground's

Authorized licensed use limited to: University of Adelaide. Downloaded on September 03,2021 at 01:20:20 UTC from IEEE Xplore. Restrictions apply.

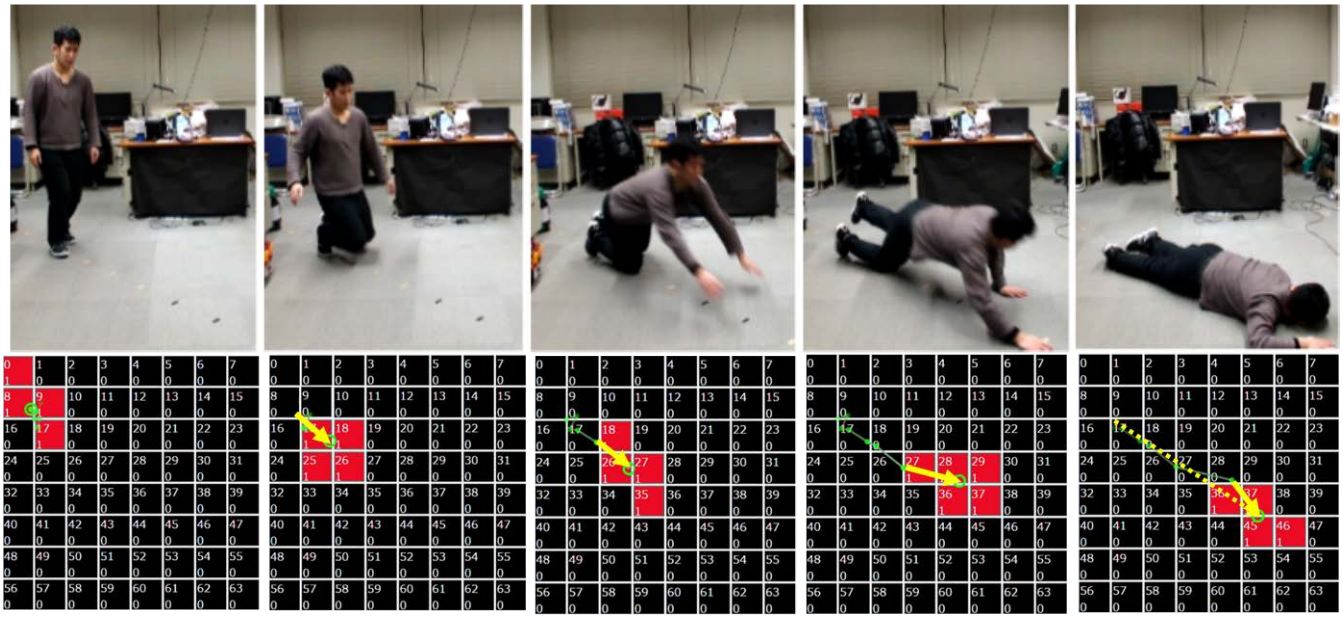

Figure 4. Snapshots of a human fall with corresponding variation of foreground region and motion distance

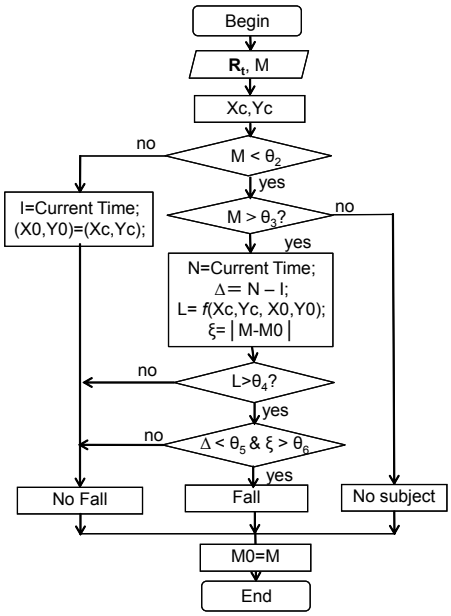

Figure 5. A flowchart of the fall detection algorithm

bounding box, modifies M0 and returns to the T-map acquisition step.

III. Implementation and Evaluation

We developed a prototype system implementation which consists of a sensor node and a PC server (HP Pro Book 450 G3, Windows 10 OS, Intel Core i3 Core i3-6100U CPU) connected by wireless Xbee protocol. The server is also

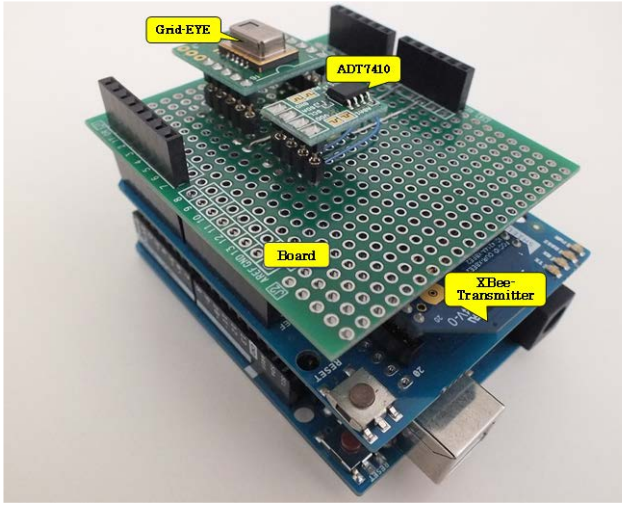

Figure 6. The sensor node

connected to the internet. The sensor node (Fig.7) is implemented on Arduino Uno Rev.3 micro-board (ATmega328 micro-controller, 32K flash memory) and has an 8x8 IR array sensor Grid-Eye AMG8831 from Panasonic [22], a temperature sensor (ADT7410), and the Xbee transmitter (placed under the sensor board) [22]. The Grid-EYE is connected to Arduino by I2C communication interface. Arduino also implements the Xbee pin-sleep control waking it up from the sleep mode only if fall is detected. The controller keeps the XBee awake for the 5s range to allow the server to react to the data sent. As a client device, we used phone (Android 6.0 OS, Qualcomm MSM8994 CPU).

Authorized licensed use limited to: University of Adelaide. Downloaded on September 03,2021 at 01:20:20 UTC from IEEE Xplore. Restrictions apply.

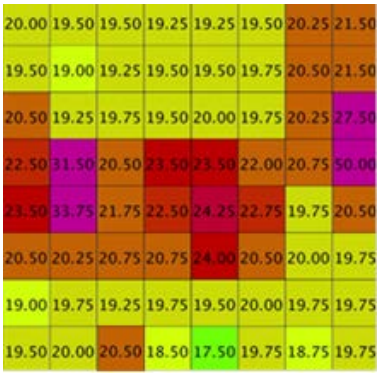

Figure 7. A T-map affected by noise from an electric heater (left side), a halogen lamp (right side) and a computer (bottom side)

The software was created by using the Microsoft Visual Studio 2013 (Eclipse 3.8.2) and the Android software development kit. The client software was developed in Java using Java-script interpreter. The fall detection alerts were displayed on the screen of the server and on the screen of a mobile phone. Each message contained a time stamp in order to evaluate the transmission delay.

To evaluate the system performance, a number of experiments have been conducted in laboratory settings. The sensor node was placed on ceiling, 2.60cm above the floor, with detection area of 2.73m×2.73m. Each experiment involved 7 participants of different heights and shapes. Each participant was asked to perform six actions (walk-in the room, stand, sit, stand, walk and fall down) ten times. The walking was at a speed of 1m/s, i.e. typical to old people. Overall, each test totaled 420 simulated actions, 70 of which were falls. The fall detection accuracy has been computed as the number correctly classified actions (fall and no-falls) to the total number of simulated actions. Standing, sitting and walking actions were categorized as a non-fall.

Our first experiment analyzed the fall detection accuracy and its dependency on the room temperature. In the experiment, we tested the system at 18ºC then incremented the room temperature by 2ºC, waited 10min for the temperature to set and then repeated the tests up to 28 ºC. Overall six tests have been carried out in this experiment. As the results (Table I) reveal, the proposed system achieves 96% fall detection accuracy at 20ºC - 22ºC irrespectively to the subject height or shape. As the room gets warmer, the smaller difference between the room temperature and the body temperature affects the system accuracy. At 28ºC, for example, the detection ratio is 87%. The total delay from detecting a fall to receiving a fall alert at the client device in the system was 0.8sec.

TABLE I. FALL DETECTION ACCURACY VS. ROOM TEMPERATURE

Activity	**Temperature (C)**					
	18º	***20º***	***22º***	***24º***	***26º***	***28º***
Fall	97%	96%	96%	94%	90%	83%
No-Fall	3%	4%	4%	7%	8%	17%

The second experiment evaluated system performance vs. thermal noise produced by electric appliances. To model such a noise, we placed three different electric devices inside the monitored area and carried the tests when each of them was switched on while the others were off and when all of the devices were switched on. The devices used included a 1500W electric heater (Technos ES-K709), a 500W Halogen lamp (WLT-280) and notebook computer (HP Pro Book 450). Fig.8 shows a T-map when all the devices were on. As one can see, these devices generate a strong noise in T-Map.

Table II summarizes the results obtained at 20ºC room temperature. By comparing them with data presented in Table I, it is obvious that the noise from the devices does not affect the fall detection accuracy of the proposed system. The system has same detection rate with and without the noise.

In the third experiment, we estimated the system performance at different room illuminance levels obtained during daytime and night time. Because the IR flux absorbed by the Grid-Eye depends on room illuminance, we expected a large impact on performance. The experiment results (measured at 11ºC - 17ºC outside temperature and 20ºC room temperature) show however that the room illuminance does not affect much the system accuracy, unless the temperature inside the room is significantly changing. As Table III shows, variation in the detection accuracy is a few percent only even in a very bright room illumination.

TABLE II . FALL DETECTION ACCURACY IN A NOISY ENVIRONMENT

Activity	**Electric devices**			
	H-lamp	***Heater***	***PC***	***All***
Fall	96%	96%	96%	96%
No-Fall	4%	4%	4%	4%

TABLE III. FALL DETECTION ACCURACY VS. ROOM BRIGHTNESS

Room Lighting	OFF	OFF	ON	ON
Sunlight	No	Yes	No	Yes
Illuminance (lx)	20-30	120	900	1000
Fall	93%	93%	96%	92%
No-Fall	7%	7%	4%	8%

Finally, we compare the data communication rates employed in related fall detection system [16] and our system. Because [16] transmits a 8bit address and a frame of 64 bytes at 20fps rate, it requires 10,250 bits of data to be sent to server every second, keeping the transmitter always active. In contrast, our system runs fall detection inside the node, sending only 9 bits of data (8 bit address and 1 bit signal) only when a fall occurs. All the other time, the transmitter is put in a low-energy sleep mode. For the same voltage supply and switching capacitance, our system is clearly less energy consuming. Furthermore, due to using less operations and data transfers, our system can put wireless transmitter into low-energy sleep mode when there no falls (i.e. most of the time). In opposite, [16] must always have the transmitter active in order to convey data to a server. For the same voltage supply and switching capacitance our system is clearly less energy consuming.

Authorized licensed use limited to: University of Adelaide. Downloaded on September 03,2021 at 01:20:20 UTC from IEEE Xplore. Restrictions apply.

IV. Conclusion

In this paper, we presented new system for unobtrusive fall detection using small IR array sensors. In comparison to existing design, the system operates at 1/4 of processing rate while employing wireless transmission only when a fall occurs. As experimental evaluation showed, the system achieves real-time and robust fall recognition rate (over 94%) at room temperatures up to 24ºC. It performs reliably in static environments and is not affected by the heat produced by other electric devices. The research presented here is a work in progress and the list of things to improve it is long. In the current study, we restricted ourselves to a simple case of singular node, with relatively small area, laboratory settings, simplified human fall modeling and abstract estimation of energy consumption. To make the technology widely accepted these limitations must be overcome. Also when talking about the fall detection in general, some critical issues arise. The people might use rooms in multi-floor households, wear warm clothes and hats. The robust real-time fall detection by sensor nodes placed on ceilings might be quite difficult. We are currently investigating these issues as well detailed measurement of energy consumption.

References

[1] World Health Organization: Global report on falls prevention in older age. 2007, accessed on internet on Feb.5, 2017 from http://www.who.int/ageing/publications/Falls_prevention7March.pdf

[2] M. Tinetti, W. Liu, and E. Claus. "Predictors and prognosis of inability to get up after falls among elderly persons". J. of the American Medical Association, vol. 269, no.1, Jan.1993, pp. 65-70.

[3] R.Igual, C.Medrano and I.Plaza, Challenges, issues and trends in fall detection systems. BioMedical Eng. OnLine, 2013, vol.12, no.66, pp.1-24

[4] M.Mubashir, L.Shao, and L.Seed. A survey on fall detection: Principles and approaches. Neurocomput. 100, pp.144-152, Jan. 2013

[5] Y.S.Delahoz and M.A.Labrador. Survey on Fall Detection and Fall Prevention Using Wearable and External Sensors, Sensors, 14, Oct. 2014, pp. 19806-19842;

[6] E.J. Porter, "Wearing and using personal emergency response system buttons: Older frail windows' intentions". J.of Gerontological Nursing, vol.31, no.10, Oct. 2005, pp.26-33.

[7] J.A.Langlois, S.R.Kegler, J.A.Gotsch, et al., "Traumatic brain injury-related hospital discharges: Results from a 14-state surveillance system", 2003, available from www.cdc.gov/MMWR/preview/mmwrhtml/ss5204a1.html

[8] Kruse, P.W. Uncooled Thermal Imaging Arrays, Systems, and Applications; SPIE: Washington, DC, USA, 2001; pp. 25–56

[9] M.Kimata. Trends in small-format infrared array sensors. In Proceedings of the Sensors, pp. 1-4, 2013;

[10] Gonzalez, L. I. L., Troost, M., & Amft, O. Using a thermopile matrix sensor to recognize energy-related activities in offices. Procedia Computer Science, 19, 2013, pp.678-685

[11] V.L.Erickson, A.Beltran, D.A. Winkler, N.P.Esfahani, J.R.Lusby, and A.E.Cerpa. "TOSS: Thermal Occupancy Sensing System." In Proceedings of the 5th ACM Workshop on Embedded Systems For Energy-Efficient Buildings, pp. 1-2. ACM, 2013.

[12] C.Basu, A.Rowe. Tracking Motion and Proxemics using Thermal-sensor Array. arXiv preprint arXiv:1511.08166. Nov. 25. 2015

[13] D.C.Kallur, Human localization and activity recognition using distributed motion sensors," M.S.Thesis, Oklahoma State University, July 2014.

[14] A.Sixsmith, N.Johnson, and R.Whatmore, Pyroelectric IR sensor arrays for fall detection in the older population, J. Phys. IV France 128, 2005, pp.153–160

[15] S.Mashiyama, J.Hong, T.Ohtsuki, Activity recognition using low resolution infrared array sensor, IEEE Int. Conf. on Communications, pp. 495-500, 2015.

[16] S. Mashiyama, J. Hong, and T. Ohtsuki, "Activity recognition using low resolution infrared array sensor," IEEE Int. Conf. on Communications (ICC'2015), London, UK, June 2015.

[17] Infrared Array Sensor Grid-EYE (AMG88). Panasonic Corp. Retrieved May 2013, available from http://pewa.panasonic.com/assets/pcsd/catalog/grid-eye-catalog.pdf

[18] XBee Buying Guide, SPARC Electronics, available from https://www.sparkfun.com/pages/xbee_guide

[19] P.Smith, Comparing Low-Power Wireless Technologies, Digi-Key Electronics, 2011-08-08, available from https://www.digikey.com/en/articles/techzone/2011/aug/comparing-low-power-wireless-technologies

[20] Arduino Power Consumption Normal & Sleep, Gadet Market, Sep.2, 2013. https://www.gadgetmakersblog.com/arduino-power-consumption/

[21] M. Piccardi. Background subtraction techniques: a review (PDF). IEEE International Conference on Systems, Man and Cybernetics. 4. pp. 3099–3104, Oct.2004

[22] Occupancy sensors: motion-sensing devices for lighting control. Specifier reports, vol.5, no.1, LRC, Rensselar Polytechnic Institute, Oct.1998.

Authorized licensed use limited to: University of Adelaide. Downloaded on September 03,2021 at 01:20:20 UTC from IEEE Xplore. Restrictions apply.